CEMENT and CONCRETE RESEARCH. Vol. 17, pp. 951-967, 1987. Printed in the USA
0008-8846/87 $3.00+00.

SNAPBACK INSTABILITY AT CRACK LIGAMENT TEARING AND ITS IMPLICATION FOR FRACTURE MICROMECHANICS

Zdeněk P. Bažant
Professor of Civil Engineering
Northwestern University, Evanston IL 60201, USA

(Communicated by F.H. Wittmann)
(Received July 13, 1987)

ABSTRACT

The microcracking in the fracture process zone ahead of a major crack is assumed to consist, in the initial stage, of a two-dimensional array of small circular (penny-shaped) cracks and, in the terminal stage, of a two-dimensional array of small circular ligaments, all located on the main crack plane. Both cases are solved in three-dimensions according to linear elastic fracture mechanics. The solution is approximate but asymptotically exact both for very small circular cracks and very small circular ligaments. The spacing of the cracks as well as the ligaments is governed by the spacing of the large aggregate pieces. The curve of the transverse displacement v due to cracks versus the remote applied normal stress is calculated and is found to exhibit snapback instability at which a negative slope changes to a positive slope and v reaches its maximum possible value. Since several other influencing physical mechanisms were neglected in the analysis, it still remains to be verified whether the snapback instability does actually occur in the concrete fracture process. The asymptotic behavior at ligament tearing is further analyzed, based on St.-Venant's principle, for arbitrary general three- and two-dimensional situations and it is shown that when the ligament transmits a force (mode I, II or III), its final tearing is always characterized by snapback instability, which determines maximum possible displacement due to crack. When, however, the ligaments transmit only a moment (bending or torsional), there is no snapback instability.

Nature of Problem

The softening law for the fracture process zone of a heterogeneous material such as concrete may be characterized either by the function $\sigma = \sigma(\delta_f)$ or the function $\sigma = \sigma(\gamma)$ where σ is the normal stress across the plane of the crack ahead of the crack tip, δ_f is the total displacement across the fracture process zone of width w_c, and $\gamma = \delta_f/w_c$ = mean normal strain across the fracture process zone (Fig. 1). The shape of the curve $\sigma(\delta_f)$ or $\sigma(\gamma)$ is the central question in the modeling of fracture in concrete as well as other materials such as rock, ceramics, composites, ice, etc. (1).

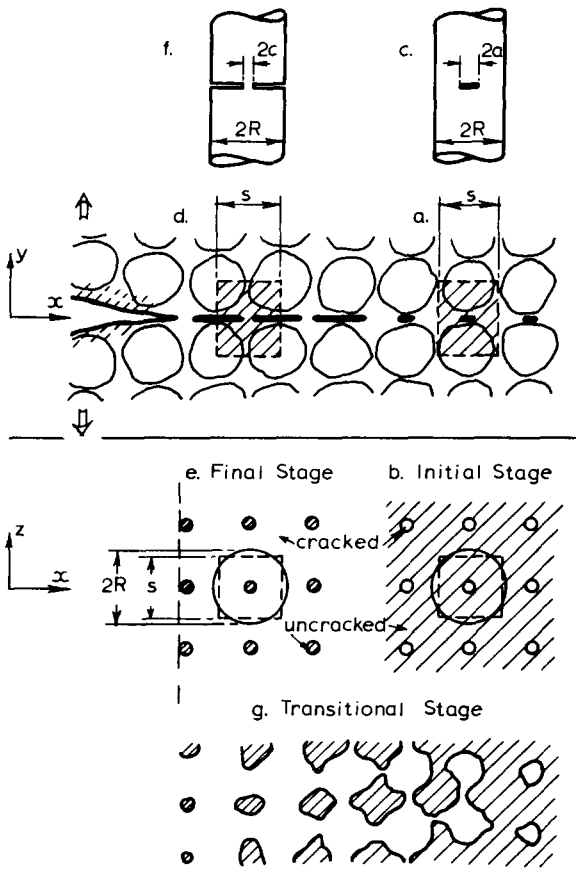

FIG. 1
Three-dimensional Idealization of the Microcracking Process Ahead of the Main Crack

The main microstructural influences on function $\sigma(\delta_f)$ or $\sigma(\gamma)$ include: 1) the nucleation, growth and coalescence of microcracks within the fracture process zone; 2) the heterogeneous microstructure, in which the difference of elastic moduli between the aggregate and the mortar matrix is the dominant feature; 3) the strength of the interfaces between the aggregate and the matrix, which is normally weaker than the strength (or fracture toughness) of either the aggregate or the matrix; and 4) various inelastic phenomena occurring away from microcrack tips, such as frictional slip, resistance to crack closure, etc It is difficult to study all these effects simultaneously. This study* will focus on effect 1 and take into account effect 2 only insofar as the spacing of microcracks is concerned. The main objective is to study the $\sigma(\delta_f)$-curve from the stability viewpoint, especially in terminal asymptotic stage of ligament tearing, on which little information exists at present.

Idealization of Crack System Initiation, Growth and Coalescence

To facilitate analysis, we imagine the array of aggregate pieces to be

*based on Report (23)

regular, organized as a cubic lattice (Fig. 1). This idealization was used before to derive from the initiation condition of interaggregate cracks a formula for the decrease of concrete strength as a function of the maximum aggregate size (1,2), which was found to agree with test results. Now we use the same idealization to study crack initiation as well as terminal coalescence.

If the aggregate is stiffer than the matrix (as is true of normal concretes), or if at least the aggregate-matrix interface is weaker, the microcracks are likely to initiate in the thin contact zones between aggregate pieces (Fig. 1a). The initiating microcracks which form in the fracture process zone ahead of the main crack (Fig. 1) may be imagined to be circular (penny-shaped), of diameter 2a. Their spacing in the plane (xz) of the main crack is the same as the spacing s of the large aggregate pieces, which may be given as $s = n_s d_a$ where d_a = maximum aggregate size and n_s = empirical factor greater than 1 but close to 1, perhaps $n_s = 1.1$.

The largest microcracks form on the main crack plane, and smaller microcracks form away from the crack plane. The reality is somewhere between the following two ideal limiting cases: 1) The microcracks arise only on the crack plane, thus forming a two-dimensional periodic array in the plane (xz); and 2) the microcracks form a three-dimensionally periodic array in space (xyz), being the same on the crack plane as well as the adjacent parallel planes.

Case 1 conforms to the classical Dugdale's and Barrenblatt's cohesive zone concept, in which all fracturing is imagined to be lumped into the crack plane. Case 2 corresponds to the more recent strain-softening models for cracking (1), which are now known to describe fracture realistically and in a theoretically consistent framework provided that the softening is treated in a nonlocal manner (3, 4). We analyze here only Case 1.

At the beginning, the cracks may be assumed to be circular (penny-shaped), of radius $a << s$ (Fig. 1a,b). Later the cracks develop complex irregular shapes in the crack plane as they gradually coalesce with each other. In the terminal stage of tearing, however, the uncracked area may be assumed to have again a simple shape, consisting of a periodic array of circular ligaments, of radius 2c, such that $c << s$ (Fig. 1 d,e).

For $a << s$, the situation may be idealized as a single penny-shaped crack within an infinite cylinder (Fig. 1c) of radius R. Force (and work) equivalence requires that the cylinder cross-section area of the cylinder be the same as one square of the lattice, i.e. $\pi R^2 = s^2$, from which $R = s/\sqrt{\pi}$. For $c << s$, the situation may be idealized as a single penny-shaped ligament of radius c within an infinite cylinder of radius $R = s/\sqrt{\pi}$ (Fig. 1d,e,f). While the linear elastic fracture mechanics does not apply to the macroscopic fracture, we may assume it to apply for the growths of the microcracks. The linear elastic solution for the penny-shaped crack (for any a(s)) was given by Bueckner (5) and Benthem (6); see Tada's handbook (7, p. 27.1). The solution for the penny-shaped ligament was given perhaps most accurately by Nisitani and Noda (8) (see Murakami's handbook (9, p. 643)), and previously by Bueckner (5), Benthem and Koiter (6), Harris (10), and others (cf. 7,9).

Circular (Penny-Shaped) Cracks: Initial Stage

For the penny-shaped crack, Benthem and Koiter (6) (see also p. 27.4 of Ref. 7 or p. 653 of Ref. 9) found that

$$K_I = \sigma\sqrt{R} f_1(\alpha), \qquad \alpha = a/R \tag{1}$$

where

$$f_1(\alpha) = \frac{2}{1-\alpha^2}\sqrt{\frac{\alpha}{\pi}(1-\alpha)}\left(1 + \tfrac{1}{2}\alpha - \tfrac{5}{8}\alpha^2 + 0.421\alpha^3\right). \tag{2}$$

K_I = Mode I stress intensity factor; $\sigma = P/\pi R^2 = P/s^2$ = average axial stress; P = resultant axial force on the cylinder (Fig. 1b). The error is under 1%. The necessary condition of propagation of the cracks is $K_I = K_{cm}$ = critical stress intensity factor of the microcracks (material constant). So the remote stress required for crack propagation is:

$$\sigma = \frac{K_{cm}}{f_1(\alpha)\sqrt{R}} . \tag{3}$$

To calculate the displacement v due to the cracks, we need to determine first the strain energy W_1 per crack that has been released due to the formation of the cracks. The energy release rate G is known to be (11, p. 108) $G = K_I^2/E'$ where $E' = E/(1-\nu^2)$, ν = Poisson ratio, E = Young's elastic modulus. By definition $\partial W_1/\partial a = 2\pi a G$, and so

$$\frac{\partial W_1}{\partial a} = 2\pi a G = 2\pi a \frac{K_I^2}{E'} = 2\pi a R \frac{\sigma^2}{E'} f_1^2(\alpha). \tag{4}$$

Integrating, with the substitutions $a = R\alpha$ and $da = Rd\alpha$, we get

$$W_1 = 2\pi R^3 \frac{\sigma^2}{E'} G_1(\alpha), \tag{5}$$

where

$$G_1(\alpha) = \int_0^\alpha \alpha' f_1^2(\alpha')d\alpha' . \tag{6}$$

The displacement at $y \to \infty$ due to the formation of the crack must, therefore, be

$$v = \frac{\partial W_1}{\partial P} = \frac{1}{\pi R^2}\frac{\partial W_1}{\partial \sigma} = 4R\frac{\sigma}{E'} G_1(\alpha). \tag{7}$$

Eqs. 3 and 7 represent a parametric description of the stress-displacement curve. Choosing various values of α, and evaluating σ and v, one obtains the plot in Fig. 2 in which S = nondimensional remote applied stress and q = nondimensional displacement due to the crack;

$$S = \sigma\frac{\sqrt{R}}{K_{cm}}, \quad q = v\frac{E'}{K_{cm}\sqrt{R}} \qquad (R = s/\sqrt{\pi}). \tag{8}$$

Small Circular Cracks: Asymptotic Approximation

An explicit, asymptotically exact solution can be obtained for the special case of small α ($\alpha \ll 1$ or $a \ll R$). Then $f_1(\alpha) = 2(\alpha/\pi)^{1/2}$, and so

$$K_I = 2\sigma\sqrt{a/\pi}. \tag{9}$$

Then $\partial W_1/\partial a = 2\pi a K_I^2/E' = 8\sigma^2 a^2/E'$. By integration, $W_1 = 8\sigma^2 a^3/3E'$. Note that in contrast to Eqs. 1, 4 and 6, these expressions are independent of R. By differentiation,

$$v = \frac{\partial W_1}{\partial P} = \frac{1}{\pi R^2}\frac{\partial W_1}{\partial \sigma} = \frac{16}{3\pi}\frac{\sigma}{E'}\frac{a^3}{R^2} = \frac{16}{3}\frac{\sigma}{E'}\frac{a^3}{s^2}, \tag{10}$$

where we used the relation $s^2 = \pi R^2$, which guarantees the force equivalence with a square grid of small circular cracks to be satisfied exactly. We see that the displacement v due to the cracks depends on R, and thus on spacing s. Setting $K_I = K_{cm}$, Eq. 9 yields $a = \pi K_{cm}^2/4\sigma^2$, and Eq. 10 becomes

$$v = \frac{\pi^2 K_{cm}^6}{12E'R^2}\frac{1}{\sigma^5} = \frac{\pi^3 K_{cm}^6}{12E's^2}\frac{1}{\sigma^5} \qquad (\sigma \le f_t') \tag{11}$$

Since the material can resist only finite stress, this equation is meaningful only for $\sigma < f_t'$ where f_t' = tensile strength. As argued already by Griffith, the creator of fracture mechanics, it follows from Eq. 9 that the material must initially contain flaws equivalent to circular cracks of radius $a = a_0$,

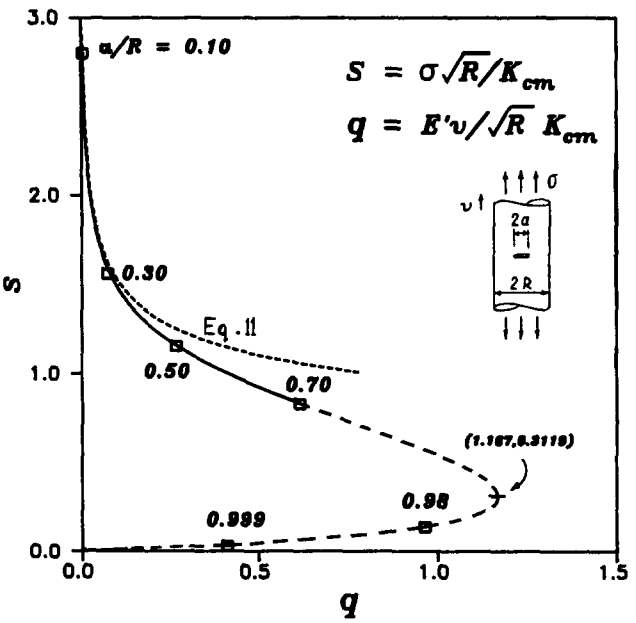

FIG. 2
Nondimensional Remote Stress vs. Nondimensional Remote Displacement Due to Cracks for the Initial State Idealization as a Circular (Penny-Shaped) Crack in a Cylinder (dashed segment, a/R > 0.70 is irrelevent since it is not initial stage).

$$a_0 = \frac{\pi}{4}\frac{K_{cm}^2}{f_t'^2} . \tag{12}$$

Although the present solution is valid only if all the initial flaws are located on one plane, the flaws are in reality distributed through the material uniformly. The initial displacement due to cracks when the cracks first become critical ($\sigma = f_t'$) then is, according to Eq. 11,

$$v_0 = \frac{\pi^3 K_{cm}^6}{12\, E' s^2 f_t'^5} . \tag{13}$$

During the initial loading from $\sigma = 0$ to $\sigma = f_t'$, the cracks do not grow ($K_I < K_{cm}$), and so the $\sigma - v$ relation is a straight line, $\sigma = C_0 v$, where $C_0 = f_t'/v_0$ = stiffness per unit area due to preexisting flaws;

$$C_0 = \frac{12}{\pi^3} E' s^2 \left(\frac{f_t'}{K_{cm}}\right)^6 . \tag{14}$$

Assuming that the effective width w_c of the fracture process zone is such that the displacement at its boundary is nearly the same as v at $y \to \infty$, the total initial displacements δ_f across the fracture process zone before the cracks become critical is

$$\delta_f = \left(\frac{w_c}{E'} + \frac{1}{C_0}\right)\sigma \qquad (\text{for } v \le v_0) \tag{15}$$

where $E' = E/(1-\nu^2)$. E must obviously be interpreted as the theoretical elastic modulus of the material without any preexisting flaws. The elastic modulus measured in a tensile test is $E_{eff} = [E'^{-1} + (C_0 w_c)^{-1}]^{-1}$. After the cracks become critical

$$\delta_f = \frac{w_c \sigma}{E'} + \frac{\pi^3 K_{cm}^6}{6E' s^2}\frac{1}{\sigma^5} \qquad (\text{for } v \ge v_0,\ a \ll s). \tag{16}$$

In analogy to Eq. 15, deformation $w_c\sigma/E'$ needs to be also added to the plot $v(\sigma)$ in Fig. 2 in order to get the plot of δ_f versus σ valid for any α.

Circular Ligaments: Terminal Stage of Crack Coalescence

Now consider the case of a penny-shaped ligament in an infinite circular cylinder of radius R. The result of elastic analysis (8,9) is:

$$K_I = \sigma\sqrt{R}\, f_2(\xi) \qquad (\xi = c/R) \tag{17}$$

where

$$f_2(\xi) = \tfrac{1}{2}\left[\frac{\pi}{\xi^3}(1-\xi)\right]^{\frac{1}{2}}\left(1 + \frac{\xi}{2} + \frac{3\xi^2}{8} - 0.363\xi^3 + 0.731\xi^4\right)(1 + 0.1\xi^2\sqrt{1-\xi}) \tag{18}$$

c = radius of ligament (Fig. 1e), $\sigma = P/\pi R^2$, and P = axial force. The remote applied stress required for crack propagation is:

$$\sigma = \frac{K_{cm}}{f_2(\xi)\sqrt{R}} \cdot \tag{19}$$

The energy release rate is

$$-\frac{\partial W_2}{\partial c} = 2\pi c\,\frac{K_I^2}{E'} = 2\pi cR\,\frac{\sigma^2}{E'} f_2^2(\xi). \tag{20}$$

By integration, with substitutions $c = R\xi$ and $dc = Rd\xi$,

$$W_2 = \int_1^{\xi} \frac{\partial W_2}{\partial c}\, dc = -\int_{\xi}^{1} \frac{\partial W_2}{\partial c}\, dc = 2\pi R^3 \frac{\sigma^2}{E'} G_2(\xi) \tag{21}$$

where

$$G_2(\xi) = \int_{\xi}^{1} \xi' f_2^2(\xi')\, d\xi'. \tag{22}$$

The displacement v at $y \to \infty$, caused by the crack, may now be calculated as

$$v = \frac{\partial W_2}{\partial P} = \frac{1}{\pi R^2}\,\frac{\partial W_2}{\partial \sigma} = 4R\,\frac{\sigma}{E'} G_2(\xi). \tag{23}$$

Eqs. 19 and 23 represent a parametric description of the stress-displacement curve. Choosing various values of ξ and evaluating σ and v, one obtains the plot in Fig. 3 in terms of nondimensional stress S and displacement q defined by Eq. 8.

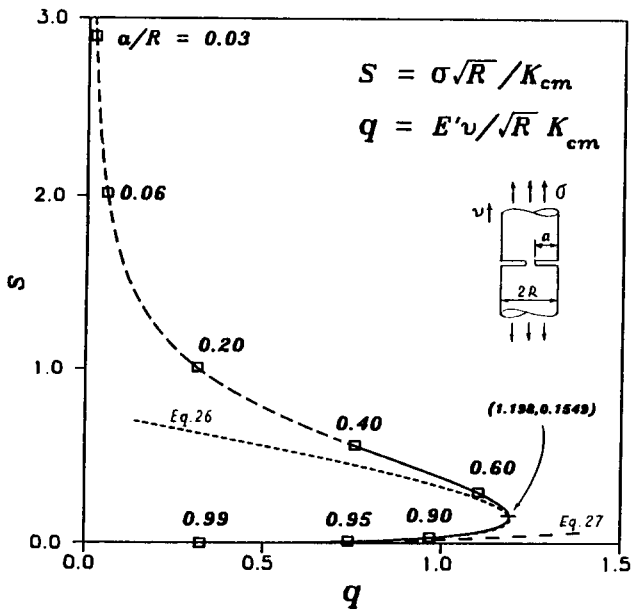

FIG. 3
Nondimensional Remote Stress vs. Nondimensional Remote Displacement Due to Crack for the Terminal State Idealization as a Circular Ligament in a Cylinder (dashed segment, a/R < 0.4, is irrelevant since it is not terminal stage).

Small Circular Ligaments: Asymptotic Approximation

An explicit asymptotically exact solution can be obtained for the special case of small ξ ($\xi << 1$ or $c << R$). Then $K_I = \frac{1}{2}\sigma(\pi R\xi^{-3})^{\frac{1}{2}}$, i.e.

$$K_I = \frac{P}{2\sqrt{\pi c^3}} . \tag{24}$$

Then $-\partial W_2/\partial c = 2\pi c K_I^2/E' = P^2/2E'c^2$. Note that, in contrast to Eqs. 17 and 20, these equations are independent of R, but only if they are written in terms of the applied force P rather than the applied stress σ (for very small cracks, Eqs. 9-10, this is true only if the equations are written in terms of σ rather than P). By integration, $W_2 = (P^2/2E')(c^{-1} - \kappa/s)$ where κ is a nondimensional integration constant. By differentiation

$$v = \frac{\partial W_2}{\partial P} = \frac{P}{E'}\left(\frac{1}{c} - \frac{\kappa}{s}\right). \tag{25}$$

Setting $K_I = K_{cm}$, Eq. 24 yields $c = (P/2K_{cm}\sqrt{\pi})^{2/3}$ and Eq. 25 then becomes

$$v = \frac{s}{E'}\left[\left(\frac{4\pi K_{cm}^2}{s\sigma^2}\right)^{1/3} - \kappa\right]\sigma. \tag{26}$$

For very small σ, we may neglect κ compared to the first term in the bracket, and we get

$$P = \sigma s^2 \simeq \frac{E'^3}{4\pi K_{cm}^2} v^3 = \frac{E'^3}{4\pi K_{cm}^2} v^3 \quad \text{(small v)}. \tag{27}$$

For Eq. 26 which applies for larger (but still small) σ-values, we need to figure out the integration constant κ. If the solution were valid up to $c = R$, it would be proper to determine κ from the condition that $W_2 = 0$ for $c = R$. The solution, however, is valid only for $c << R$, and so we need some other condition to determine κ.

For any $\kappa > 0$, the curve $v(\sigma)$ according to Eq. 26 obviously has a point of maximum v. For arbitrary κ, this maximum point does not coincide with the exact maximum point in Fig. 3 based on Eqs. 19 and 23. Assuming that the point of v_{max} in Fig. 3 is still in the range of small enough c, we may determine κ from the condition that the graph of Eq. 26 would pass through the exact point of v_{max}, which is characterized by $S_{cr} = 1.198$ and $q_{max} = 0.1549$ (Fig. 3). Then, according to Eq. 8, $v_{max} = q_{max}K_{cm}\sqrt{R}/E'$ and $\sigma_{cr} = S_{cr}K_{cm}/\sqrt{R}$, and setting $v = v_{max}$, $\sigma = \sigma_{cr}$, Eq. 26 yields:

$$\kappa = \left(\frac{4\pi K_{cm}^2}{s\sigma_{cr}^2}\right)^{1/3} - \frac{E'}{s}\frac{v_{max}}{\sigma_{cr}} = \left(\frac{4\sqrt{\pi}}{S_{cr}^2}\right)^{1/3} - \frac{q_{max}}{S_{cr}\sqrt{\pi}} = 2.299 \tag{28}$$

Similar to the arguments related to Eqs. 14-16, the total displacement over the width w_c of the fracture process zone is, approximately,

$$\Delta_f = \left\{\frac{w_c}{E'} + \frac{s}{E'}\left[\left(\frac{4\pi K_{cm}^2}{s\sigma^2}\right)^{1/3} - \kappa\right]\right\}\sigma. \tag{29}$$

Interpretation of Mathematical Results

Although the displacement v due to cracks has been calculated for points infinitely far away from the crack plane, the displacement δ_{cr} due to cracking which arises over the finite width w_c of the fracture process zone must be nearly the same, i.e. $\delta_{cr} \simeq v$. This is indicated by some solutions for interacting cracks on parallel planes at spacing s, which are available in the literature. E.g., the problem of interacting circular ligaments of diameter 2c and

spacing h in an infinite cylinder of radius R has been solved by Nisitani and Noda (8). Their results show that the interaction of cracks causes K_I to change by less than 1% if $h \geq R$ (see p. 644 of Ref. 9). For the planar problem of an infinite stack of parallel cracks of length 2a and spacing h between the crack planes, Yokobori and Ichikawa (cf. p. 202 of Ref. 9) found the crack interaction to cause a change of K_I by less than 1% if $2a < 0.08h$, and less than 10% if $2a < 0.21h$. Although Nisitani and Noda's solution is limited to $c/h \leq 0.5$, one can nevertheless invoke St.-Venant's principle to conclude that interaction of cracks on parallel planes of spacing s should be insignificant when approximately either $a \leq h/5$ or $c \leq h/5$. Since for concrete h must be about the same as s, the preceding solutions are asymptotically exact for crack initiation ($a << h$) as well as for terminal crack coalescence ($c \leq h$). So we may interpret v as the additional displacement across the fracture process zone due to the cracks, provided that all the cracks occur on one plane.

The most interesting feature of our results is the fact that the softening stress-displacement diagram $v(\sigma)$ exhibits a maximum displacement v_{max} after which both v and σ must decrease. This behavior is known in stability theory as the snapback instability. It means that, according to the present mathematical model, the ligament tearing cannot be stable even in a displacement-controled test after the critical state of v_{max} is attained. This conclusion, when first reached by the writer in March 1987, appeared to conflict with the current generally accepted softening models and thus to cast doubt on the assumptions of the present analysis. A stress-displacement diagram $v(\sigma)$ which declines with a negative slope all the way to a zero stress is widely used in the present practice of finite element fracture analysis of concrete, is embodied in Hillerborg's fictitious crack model (12,1) and is also implied indirectly in the crack band model (13,14,1). This present practice has apparently been also corroborated by extensive experimental evidence, particularly the measurements of the softening stress-displacement diagrams by Reinhardt and Cornelissen (15), Petersson et al. (16), Shah et al. (17), Willam et al. (18), Wecharatana (19) and others. Some of these tests included very large crack displacements, which exceeded 20-times the displacement v_p at peak stress and corresponded to a reduction of stress to less than 5% of its peak value. Yet the test specimens remained stable and no snapback instability has been reported.

During the discussion at the RILEM-SEM International Conference on Fracture of Concrete and Rock in Houston (June 1987), however, it has transpired that the experimentalists themselves have doubts about the interpretation of their test results, particularly the way the additional displacement due to cracking, accumulated over the fracture process zone, should be determined from measurements. The possibility of different interpretations of the test results then finally encouraged writing and publishing of this paper.

It has been very gratifying to the writer to learn in June 1987 that H. Horii et al. (20), studying concrete fracture, as well as M. Ortiz (21) studying ceramic composites, obtained a similar result independently. They discovered the snapback instability on the curve $\sigma(v)$ by modeling the fracture process zone ahead of the main crack as an infinite row of identical uniformly spaced line cracks on the extension line of the main crack. The plots of $v(\sigma)$ that they obtained look similar to that in Fig. 3. Their analyses, however, were planar (two-dimensional). This would be fully realistic only if the cracks ahead of the frontal edge of the main crack had the shape of infinite strips parallel to the frontal edge (in the z-direction, Fig. 1) and normal to the plane (xy) in which the problem is analyzed. Such crack strips, however, do not appear to be very realistic for concrete, especially for the initial

stage of small cracks as well as the final stage of small ligaments between the crack tips.

Due to the three-dimensional nature of the aggregate framework, the spacing of the initial small cracks, located in the contact layers between the adjacent aggregate pieces, is certain to be about the same in the direction x of fracture propagation and in the direction z normal to it (in the crack plane xz); see Fig. 1b. The same must be true for the final stage of very small ligaments, as is clear from Fig. 1e. So one may conclude that the three-dimensional model of small circular cracks should be more realistic. In this regard it may be also noted that, in a previous analysis (2,1) the assumption that the crack spacing is determined by the aggregate spacing gave a realistic and experimentally corroborated result for the dependence of concrete strength f_t' on the aggregate size.

The fracture energy G_f of concrete is equal to the cross-hatched area 023460 in Fig. 5a which is enclosed by the complete stress-displacement curve $\sigma(v)$. The softening curve $\sigma(v)$ begins at the tensile strength limit f_t'. Since infinitely small microcracks propagate only at infinitely large stress σ (Eq. 3), there must initially exist in the material certain microcracks of finite size a_0, as already mentioned (Eq. 12). The initial loading up to the strength limit occurs without any crack growth and is, therefore, elastic, described by the initial straight line (02 in Fig. 5a). In the line-crack models of the fracture process zone, such as Hillerborg's, the stress-displacement curve which describes fracture is assumed to start on the vertical axis at point f_t', and so the crack displacement δ_{cr} to be used in Hillerborg's model must be understood as $\delta_{cr} = v - \sigma/K$ where K is such that $v(f_t') - f_t'/K = 0$, i.e. $K = f_t'/v(f_t')$.

Since cracks neither extend nor shorten during unloading, the unloading path from any point on the $\sigma(v)$ curve (Fig. 5a) is a straight line toward the origin (Fig. 5a).

When stress σ is controlled, the crack becomes unstable at the peak-stress point f_t' (point 2 in Fig. 5a). When the displacement is controlled, the crack becomes unstable when the curve $\sigma(w)$ attains a vertical tangent ($\partial\sigma/\partial w = 0$); w is the load-point displacement, $w = v + \sigma/C$ where C is the elastic stiffness of the structure without the cracks, and v is the additional displacement due to the cracks. The higher the value of C, the smaller is the stress σ_{cr} at the snapback instability. The smallest σ_{cr} is obtained for $C \to \infty$, which coincides with the σ_{cr} value for the curve $\sigma(v)$ (Fig. 3). If the displacement is controlled, the stress after the snapback instability drops instantly to 0. This drop is called the snapdown. The snapdown path is dynamic and the motion is accelerated. The energy corresponding to the cross-hatched area 0454 to the left of the snapdown path in Fig. 5b is converted into kinetic energy, which is emitted as the energy of a sound wave (acoustic emission). In fact, the existence of sound emissions in a displacement-controlled fracture test implies the occurrence of snapback.

To conduct an approximate analysis in a static manner, the equilibrium snapback path (40 in Fig. 5a) must be replaced by a $\sigma(v)$-diagram that is equivalent in terms of energy. Thus, the equivalent $\sigma(v)$ diagram for static finite element analysis must preserve the correct area G_f enclosed by the $\sigma(v)$ curve, as indicated either by the vertical snapdown path 367 in Fig. 5c or the gradual equivalent softening path 89 in Fig. 5d. If static analysis is conducted on the basis of the actual snapdown path $\overline{45}$ in Fig. 5c, the results are incorrect in terms of energy, thus violating the most fundamental requirement of mechanics.

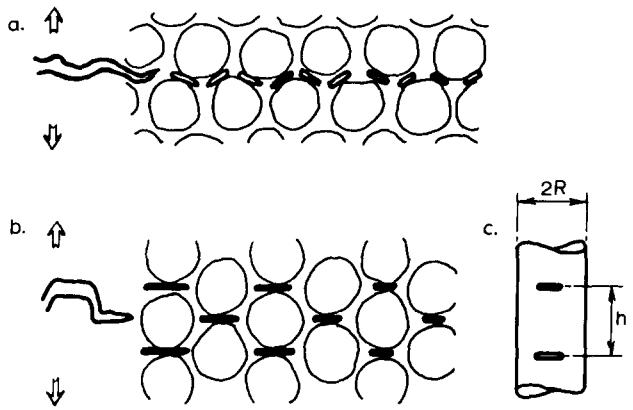

FIG. 4
Crack Systems Expected for Other Aggregate Configurations

The energy-equivalent snapdown along the vertical path 367 in Fig. 5 can actually occur only if a dynamic disturbance at point 3 imparts to the system a kinetic energy that is at least equal to the area 3463 (per unit length of fracture). Area 3463 is equal to the loss of kinetic energy along the path from point 3 to point 6 in Fig. 5c. Along the path 67 the kinetic energy is increased by an amount equal to the area 0760. The system ends at point 7 with the same kinetic energy as it had at point 3 if the areas 3463 and 0760 are equal, which is true if the area 02370 is equal to G_f.

It must be admitted that certain elastic fracture mechanisms which are neglected in the present analysis could considerably alter the shape of the $v(\sigma)$ curve including the snapback instability. These include: 1) inclination of the main crack with regard to a cubic lattice of aggregate; 2) other types of periodic lattices, e.g. of tetrahedral type (Fig. 4a,b); 3) random arrangement of aggregate pieces, which is of course the rule rather than an exception. Irregular random aggregate arrangements prevent the cracks to be all located on a single plane, contrary to the assumption of the present analysis. This has for consequence that the crack edges have not only a Mode I stress intensity factor, but also Mode II and Mode III (i.e. shear) stress intensity factors, and may therefore propagate in directions that are inclined with regard to the main crack plane (Fig. 4a). It remains to be seen whether such mechanisms can significantly alter the shape of the $v(\sigma)$ curve, especially the value of v_{max}.

The shape of the $v(\sigma)$-curve could be also significantly influenced by various inelastic phenomena. These include: 1) resistance to a crack closing due to fragmentation debris located in the crack space; 2) frictional slip on inclined cracks (Fig. 4a); and 3) irreversible deformations taking place elsewhere than microcrack tips. Since along the snapback path (40 in Fig. 5a) the portion of the crack that has formed previously is closing, the resistance to crack closing may significantly alter the snapback path and prevent complete recovery of displacement v as $\sigma \to 0$ (i.e., prevent return to point 0 in Fig. 5a). If crack closing is prevented completely, then there is no equilibrium path after the critical state of snapback (point 4, Fig. 5a) and the system can only follow the dynamic snapdown path (45 in Fig. 5b). But for reasons of stability it must follow this path anyway, and so a prevention of crack closing does not seem to alter the essential behavior.

It should also be recognized that the difference in elastic moduli between the matrix and the aggregate, as well as the fact that the microcrack fracture

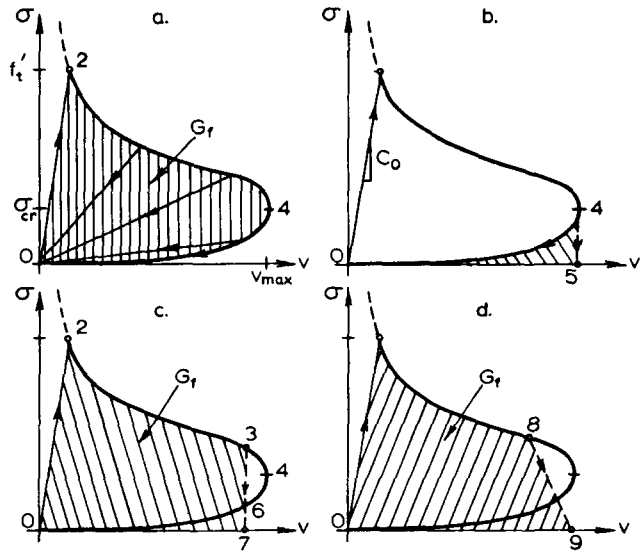

FIG. 5
Stress-Displacement Diagrams for Fracture Process Zone Modeling and Meaning of Fracture Energy.

toughness K_{cm} is probably lower at the aggregate-mortar interfaces than inside the matrix or the aggregate, has not been taken into account in the present analysis.

General Asymptotic Analysis for Small Ligament Transmitting Force or Moment

We will now show that snapback instability is a general characteristic of crack coalescence or terminal stage of crack ligament tearing in three as well as two dimensions. We consider the ligament size to be infinitely small compared to any cross section dimension of the structure. We assume the subsequent ligament shapes to be similar. Let P and M be the internal force of any direction and the internal moment about any axis transmitted across the ligament. (The special cases of P include a normal force or a shear force, and of M a bending moment or a twisting moment.) According to St.-Venant's principle, P or M can produce significant stresses and significant strain energy density only in a three-dimensional region whose size (L_1 and L_2 in Fig. 6) is of the same order of magnitude as the ligament size c. The strain energy produced in this region by P or M is

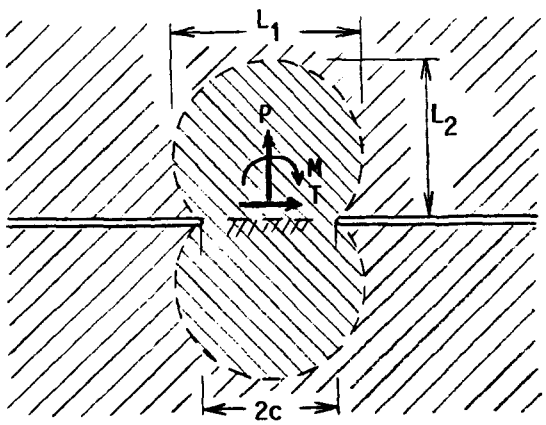

FIG. 6
Ligament Joining Two Halfspaces or Halfplanes

$$U_1 = \frac{P^2}{2EA} k_1 c = \frac{P^2}{2Ek_3 c}, \qquad U_2 = \frac{M^2}{2EI} k_2 c = \frac{M^2}{2Ek_4 c^3} \tag{30}$$

where $A = k_5 c^2$ = cross section area

of the ligament, $I = k_6 c^4$ = moment of inertia of the cross section of the ligament, and $k_1, k_2, \ldots, k_6$ = constants. The remote displacement v and rotation θ associated with P and M, respectively, are

$$v = \frac{\partial U_1}{\partial P} = \frac{P}{Ek_3 c}, \qquad \theta = \frac{\partial U_2}{\partial M} = \frac{M}{Ek_4 c^3}. \tag{31}$$

The energy release rates due to P and M per unit circumference of the ligament cross section are:

$$G_1 = -\frac{1}{k_7 c}\frac{\partial U_1}{\partial c} = \frac{P^2}{2Ek_3 k_7 c^3}, \qquad G_2 = -\frac{1}{k_8 c}\frac{\partial U_2}{\partial c} = \frac{3M^2}{2Ek_4 k_8 c^5}. \tag{32}$$

Setting $G_1 = G_f$ or $G_2 = G_f$ where $G_f = K_c^2/E$ = fracture energy of the material (a constant), we have:

$$\text{for P:}\quad c = \left(\frac{P^2}{2Ek_3 k_7 G_f}\right)^{1/3}; \qquad \text{for M:}\quad c = \left(\frac{3M^2}{2Ek_4 k_8 G_f}\right)^{1/5}. \tag{33}$$

Substituting this into Eq. 31 we get, for very small ligament size c, the asymptotic approximations:

$$\text{for P:}\quad v = c_1 P^{1/3}; \qquad \text{for M:}\quad \theta = c_2 M^{-1/5} \tag{34}$$

where c_1, c_2 = constants. Note that Eq. 34 for P agrees with Eq. 27 that we derived before in a different manner.

From Eq. 34 we conclude that for force loading of the ligament the curve v(P) must return to the origin (v = P = 0) as $P \to 0$ ($c \to 0$). This means that there must be a snapback at some finite P-value.

On the other hand, for moment loading of the ligament, the curve $\theta(M)$ tends to infinity as $M \to 0$ ($c \to 0$). So there can be no snapback.

For two-dimensional problems a similar asymptotic analysis is possible, but only for the moment loading. We have $I = k_6 bc^3$ where b = thickness of the body, and instead of Eqs. 30-32 we get

$$U_2 = \frac{M^2}{2EI} k_2 c = \frac{M^2}{2Ek_4 bc^2} \tag{35}$$

$$\theta = \frac{\partial U_2}{\partial M} = \frac{M}{Ek_4 bc^2} \tag{36}$$

$$G_2 = -\frac{\partial U_2}{\partial c} = \frac{M^2}{Ek_4 bc^3}. \tag{37}$$

Setting $G = G_f$, we have $c = (M^2/G_f E k_4 b)^{1/3}$, and substituting this into Eq. 36, we get, for small c:

$$\theta = c_2 M^{-1/3}. \tag{38}$$

So for moment loading in two dimensions there cannot be any snapback either.

For two-dimensional problems in which the ligament is loaded by a force, the foregoing approach fails because, as it turns out, the curve v(P) is not of a power type as $P \to 0$. For a sufficiently short ligament, the stress field must be the same as that near a ligament joining two elastic halfplanes. For that problem it is known that $K_I = (P/b)(2/\pi c)^{1/2}$ where P = normal (centric) force and c = half-length of the ligament (Fig. 6). Therefore $-\partial W/\partial c = bG = bK_I^2/E' = 2P^2/\pi E' bc$, and by integration the total strain energy release is:

$$W = -\frac{2P^2}{\pi E' b} \ln \frac{c}{c_0} \tag{39}$$

where c_0 = integration constant. Furthermore,

$$v = -\frac{\partial W}{\partial P} = -\frac{4P}{\pi E' b}\,\ell n\,\frac{c}{c_0}. \tag{40}$$

Setting $K_I = K_c$ = critical value of K_I, we also have $c = 2P^2/\pi b^2 K_c^2$ and substitution into Eq. 40 yields

$$v = -\frac{4P}{\pi E' b}\,\ell n\,\frac{2P^2}{\pi b^2 K_c^2 c_0} \tag{41}$$

The curve v(P) described by this equation is not of a power type, which explains why the type of approach used in Eqs. 30-38 would fail. The curve v(P) obviously exhibits a snapback since, for $P \to 0$, $\lim v = 0$. The critical state is characterized by the condition $\partial v/\partial P = 0$, which yields the critical value $P_{cr} = (\pi c_0/2)^{1/2} K_c b/e$, from which $v_{max} = (2c_0/\pi)^{1/2} K_c/E'e$.

From the fact that ligament tearing in Mode I or II or III always exhibits snapback if the force across the ligament is nonzero it follows that the stress-displacement curve for the microcrack patterns in Fig. 4 must, too, terminate with a snapback.

Conclusions

1. To model the fracture process zone of a heterogeneous brittle material such as concrete, it may be assumed that the initial stage of cracking consists of a two-dimensional array of small circular (penny-shaped) cracks in the plane of the main crack, and the final stage consists of a two-dimensional array of small circular ligaments. Both cases may be approximately solved from the known value of the Mode I stress intensity factor for a penny-shaped centrally located transverse crack in an axially loaded long cylinder, and a small circular ligament in such a cylinder. These solutions may be considered to be asymptotically exact for very small cracks or for very small ligaments.

2. The spacing of the initial small circular cracks as well as the final circular ligaments may be considered to be determined by the spacing of the large aggregate pieces in concrete.

3. The solution indicates that the curve of the additional transverse displacement v due to the crack versus the remote normal stress σ exhibits a softening segment which does not descend all the way to zero stress, as assumed in the current fracture models, but terminates with a critical state of snapback instability at which the curve $\sigma(v)$ has a vertical tangent (Fig. 5). The displacement at this critical state, v_{max}, is the maximum possible displacement due to the cracks. After this critical state, the equilibrium path $\sigma(v)$ approaches the origin as a cubic parabola with a positive slope. This postcritical path is unstable and a dynamic snapdown occurs in reality (Fig. 5b). For approximate static analysis an energy-equivalent softening path without snapback (Fig. 5c,d) needs to be introduced.

4. The present calculation of the stress-displacement curve neglects: 1) the situation in which the cracks are inclined and are loaded in Modes II and III; 2) possible strong interactions between adjacent cracks (other than those meeting at the same ligament); 3) the effect of the differences of elastic moduli between the aggregate and the matrix; 4) the fact that the aggregate-matrix interface may be weaker than the adjacent solid material; 5) the resistance to crack closing due to fragments located in the crack space; and 6) the inelastic phenomena taking place elsewhere than microcrack tips. It remains to be determined whether the essence of the preceding theoretical conclusions remains valid if all these phenomena are taken into account.

5. General asymptotic analysis shows that when the crack ligament transmits a force, its final tearing is always characterized by snapback instability and

there exists a maximum displacement. When, however, the ligament transmits only a moment, there is no snapback instability and the rotation due to the applied moment grows beyond any bounds. These conclusions are valid for three-dimensional as well as two-dimensional situations, for normal as well as shear forces, and for moments about any axis, bending as well as torsional (i.e., for Modes I, II and III).

Acknowledgment. - Grateful appreciation is due to the Air Force Office of Scientific Research for financial support under Contract No. F49620-87-C-0030DEF with Northwestern University, monitored by Dr. Spencer T. Wu. Thanks are also due to Graduate Research Assistants M. Tabbara and F.-B. Lin for help in computer plotting.

Appendix. - Stability of Three-Point Bent Specimen

The stability analysis of crack ligament tearing is not only of interest for micromechanics-based modeling of the fracture process zone, but also for various macroscopic problems. To illustrate and corroborate the general conclusions based on St.-Venant's principle, in particular Eq. 38, consider as an example the three-point bent beam specimen (Fig. 7), for which L = span, h = beam depth, a = length of crack (or of crack plus notch), c = h - a = length of ligament, b = beam thickness. In the literature there exist for this specimen various approximate K_I-formulas. However, those which are often used are invalid for small a/h. Nevertheless, a formula which is valid for the entire range $0 < a/h < 1$, is asymptotically exact for $c \to 0$, and generally has an error under 0.5%, has been derived by Srawley (22) for the case L = 4h:

$$K_I = \frac{3PL}{2bh^2}\sqrt{\pi a}\,F_1(\alpha), \qquad F_1(\alpha) = \frac{1.99 - \alpha(1-\alpha)(2.15 - 3.93\alpha + 2.7\alpha^2)}{(1+2\alpha)(1-\alpha)^{3/2}} \tag{42}$$

where $\alpha = a/h$. The rate of release of the total strain energy W of the whole specimen is

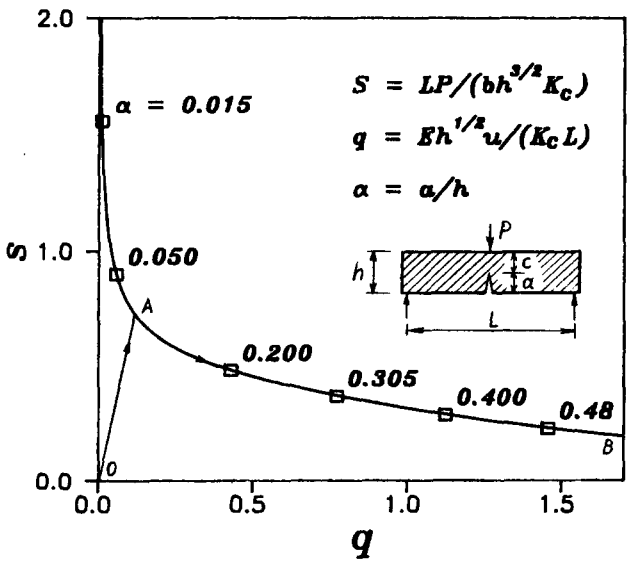

FIG. 7
Nondimensional Stress-Displacement Diagram Calculated for the Three-Point Bent Beam Specimen.

$$\frac{\partial W}{\partial a} = b\,\frac{K_I^2}{E} = \frac{9\pi}{4bE}\,\frac{P^2L^2}{h^3}\,\alpha F_1^2(\alpha). \tag{43}$$

By integration

$$W = \int_0^a \frac{\partial W}{\partial a}\,da = \int_0^\alpha \frac{\partial W}{\partial \alpha}\,h\,d\alpha = \frac{9\pi}{4bE}\,\frac{P^2L^2}{h^2}\,F_2(\alpha) \tag{44}$$

in which

$$F_2(\alpha) = \int_0^\alpha \alpha' F_1^2(\alpha')d\alpha'. \tag{45}$$

The deflection v under the load may now be calculated as

$$v = \frac{\partial W}{\partial P} = \frac{9\pi}{2bE}\,\frac{PL^2}{h^2}\,F_2(\alpha). \tag{46}$$

If the crack is propagating, we must have $K_I = K_c$ = critical value of K_I (i.e., fracture toughness of the material). Thus, Eq. 1 yields:

$$P = \frac{2bK_c}{3\sqrt{\pi}}\,\frac{h^{3/2}}{L\sqrt{\alpha}\,F_1(\alpha)}\,. \tag{47}$$

Defining the nondimensional load S and the nondimensional displacement q,

$$S = \frac{L}{K_c bh^{3/2}}\,P, \qquad q = \frac{E\sqrt{h}}{K_c L}\,u \tag{48}$$

we have from Eqs. 7 and 6:

$$S = \frac{2}{3\sqrt{\pi\alpha}\,F1(\alpha)}\,, \qquad q = 3\sqrt{\frac{\pi}{\alpha}}\,\frac{F_2(\alpha)}{F_1(\alpha)}\,. \tag{49}$$

The last equations represent a parametric definition of the non-dimensional load-deflection diagram S(q). Evaluation of S and q for various α-values yields the diagram in Figs. 7 or 8. We see that indeed there is no snapback, as indicated already by Eq. 38. The extent to which the actual measured P(v) diagram in the three-point bent test deviates from the shape in Fig. 8 is an indication of inelastic behavior and existence of a large fracture process zone.

Consider now the asymptotic behavior for small ligament, $c/h \to 0$. For that case Eq. 42 simplifies to the form:

$$K_I = 0.995(PL/b)(\pi/h^3)^{1/2}\xi^{-3/2} \qquad (\xi = c/h). \tag{50}$$

Using $\partial W/\partial \xi = -h\,\partial W/\partial a = -hbK_I^2/E$, and integrating, we get $W = 3.11\,P^2L^2\xi^{-2}/(2bh^2E)$, from which

$$v = \partial W/\partial P = 3.11\,PL^2\xi^{-2}/(bh^2E). \tag{51}$$

Setting $K_I = K_c$ and solving ξ from Eq. 50, Eq. 51 becomes

$$v = (1.45/E)(b^2K_c^2L/\pi)^{2/3}\,P^{-1/3}. \tag{52}$$

Exponent -1/3 agrees with Eq. 38 derived before for two-dimensional moment loading in general.

For very small α, $v \sim P^{-6}$, as can be verified from Eqs. 46-47.

References

1. Z.P. Bazant, "Mechanics of Distributed Cracking," Applied Mechanics Reviews 39 (5), 675 (1986).

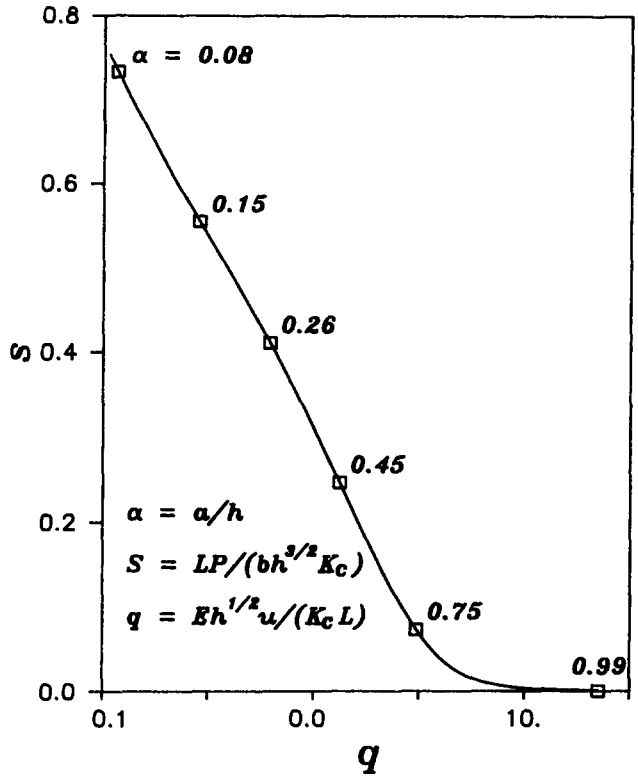

FIG. 8
Same as Fig. 7 but in Semilogarithmic Scale

2. Z.P. Bažant and J.-K. Kim, Discussion closure to the paper "Size Effect in Shear Failure of Longitudinally Reinforced Beams," ACI Journal 82 (4), 581 (1985).
3. G. Pijaudier-Cabot and Z.P. Bažant, "Nonlocal Damage Theory," Report No. 86-8/428n, Center for Concrete and Geomaterials, Northwestern University, Evanston, IL; also J. of Engng. Mechanics ASCE (1986).
4. Z.P. Bažant and G. Pijaudier-Cabot, "Modeling of Distributed Damage by Nonlocal Continuum with Local Strain," Preprints, 4th Intern. Conf. on Numerical Methods in Fracture Mechanics," ed. by A.P. Luxmore, R.J. Owen (U. of Wales, Swansea, U.K.) and M.F. Kanninen (Southwest Research Inst., San Antonio), held in San Antonio, Texas (1987), pp. 411-432.
5. H.F. Bueckner, Discussion of the paper by P.C. Paris and G.C. Sih, "Stress Analysis of Cracks," Fracture Toughness Testing and Its Applications, ASTM-STP 381, 82 (1965).
6. J.P. Benthem and W.T. Koiter, Mechanics of Fracture 1, Method of Analysis and Solutions of Crack Problems, ed. by G.C. Sih, Noordhoff Intern. Publishing, Leyden, 131-178 (1973).
7. H. Tada, P.C. Paris and J.K. Irwin, "The Stress Analysis of Cracks Handbook," 2nd ed., Paris Productions Inc., 226 Woodbourne Dr., St. Louis, Mo. (1985).
8. H. Nisitani and N. Noda, "On the Tension of a Cylindrical Bar Having an Infinite Row of Circumferential Cracks," Trans. Japan Soc. Mech. Engrs. 50 (543), 847 (1984).

9. Y. Murakami, Ed., Stress Intensity Factors Handbook, Pergamon Press, Oxford-New York (1987).
10. D.O. Harris, "Stress Intensity Factors for Hollow Circumferentially Notched Round Bars," Trans. ASME, Ser. D, J. Basic Engng. 89, 49 (1967).
11. J.F. Knott, Fundamentals of Fracture Mechanics, Butterworth, London (1983).
12. A. Hillerborg, M. Modéer and P.E. Petersson, "Analysis of Crack Formation and Crack Growth in Concrete by Means of Fracture Mechanics and Finite Elements," Cement Concr. Res. 6 (6), 773 (1976).
13. Z.P. Bažant, "Instability, Ductility and Size Effect in Strain-Softening Concrete," J. Eng. Mech. ASCE 102, 331 (1976); discussions, 103, 357, 104, 501, based on Struct. Eng. Rep. No. 74-8/640, Northwestern University, Aug. 1974.
14. Z.P. Bažant and B.H. Oh, "Crack Band Theory for Fracture of Concrete," Mat. Construct. 16 (93), 155 (1983).
15. R. Ballarini, S.P. Shah and L.M. Keer, "Crack Growth in Cement Based Composites," Eng. Fract. Mech. 20 (3) (1984).
16. P.E. Petersson, Crack Growth and Development of Fracture Zones in Plain Concrete and Similar Materials, doctoral dissertation, Lund Inst. of Tech.
17. V.S. Gopalaratram and S.P. Shah, "Softening Response of Plain Concrete in Direct Tension," ACI Journal 82 (3), 310 (1985).
18. K.J. Willam, B. Hurlbut and S. Sture, "Experimental, Constitutive and Computational Aspects of Concrete Failure" in Preprints, U.S.-Japan Seminar on Finite Element Analysis of Reinforced Concretes, Tokyo, pp. 149-172 May (1985).
19. M. Wecharatana, Paper orally presented at SEM-RILEM Intern. Conf. on Fracture of Concrete and Rock, Houston, June (1987).
20. H. Horii, A. Hasegawa and F. Nishino, "Process Zone Model and Influencing Factors in Fracture of Concrete," Preprints, SEM-RILEM Intern. Conf. on Fracture of Concrete and Rock, Houston (1987), ed. by S.P. Shah and S.E. Swartz, publ. by Soc. for Exper. Mechanics, pp. 299-307 (1987).
21. M. Ortiz, "Microcrack Coalescence and Macroscopic Crack Growth Initiation in Brittle Solids," manuscript prepared at Brown University and privately communicated to Bažant in June 1987; also Int. J. of Solids and Structures, in press.
22. J.E. Srawley, "Wide Range Stress Intensity Factor Expression for ASTM E399 Standard Fracture Toughness Specimen," Int. J. of Fract. Mech. 12, 475 (1976).
23. Z.P. Bažant, "Snapback Instability at Crack Ligament Tearing and Its Implication for Fracture Micromechanics," Report No. 87-6/498s, Center for Concrete and Geomaterials, Northwestern University, June (1987).